Non-Orthogonal Signal Transmission Over Nonlinear Optical Channels

Tongyang Xu[1], Member, IEEE, Tianhua Xu[2,3,4], Member, IEEE,
Polina Bayvel[4], Fellow, IEEE, Izzat Darwazeh[1], Senior Member, IEEE

[1]Communications and Information Systems Group, Department of Electronic & Electrical Engineering, University College London (UCL), London, WC1E 7JE, UK
[2]School of Precision Instrument & Opto-Electronics Engineering, Tianjin University, Tianjin, 300072, China
[3]School of Engineering, University of Warwick, Coventry, CV4 7AL, UK
[4]Optical Networks Group, Department of Electronic & Electrical Engineering, University College London (UCL), London, WC1E 7JE, UK

Manuscript received January 26, 2019; revised February 23, 2019; accepted March 7, 2019. Date of publication XXXX, 2019; date of current version XXXX, 2019. This work was supported by UK EPSRC program TRANSNET (EP/R035342/1), UK EPSRC program Impact Acceleration Discovery to Use Award (EP/R511638/1) and EU Horizon 2020 Marie Sklodowska-Curie RISE program (No. 778305). Corresponding author: Tianhua Xu (e-mail: tianhuaxu@outlook.com).

Abstract: The performance of spectrally efficient frequency division multiplexing (SEFDM) in optical communication systems is investigated considering the impact of fiber nonlinearities. Relative to orthogonal frequency division multiplexing (OFDM), sub-carriers within SEFDM signals are packed closer at a frequency spacing less than the symbol rate. In order to recover the data, a specially designed sphere decoding detector is used at the receiver end to compensate for the self-created inter carrier interference encountered in SEFDM signals. Our research demonstrated the benefits of the use of sphere decoding in SEFDM and also demonstrates the performance improvement of long-haul optical communication systems using SEFDM compared to the use of conventional OFDM, when fiber nonlinearities are considered. Different modulation formats ranging from 4QAM to 32QAM are studied and it is shown that, for the same spectral efficiency and information rate, SEFDM signals allow a significant increase in the transmission distance compared to conventional OFDM signals.

Index Terms: spectrally efficient frequency division multiplexing (SEFDM), orthogonal frequency division multiplexing (OFDM), optical fiber communication, nonlinear fiber channel.

1. Introduction

Optical fiber communication systems carry over 95% of the Internet data and form the major part of current communication infrastructure. Achievable spectral efficiency (SE), a figure of merit in coded communication systems, is considered a key parameter of optical fiber networks, which highlights the efficiency of optical bandwidth use [1]. With the compensation of linear transmission impairments using digital signal processing, the achievable spectral efficiency of optical communication systems is currently limited by the nonlinear distortions due to fiber Kerr effects, where signal degradation is more significant for systems using larger transmission bandwidths, closer channel spacing or higher-order modulation formats.

Multiple sub-carrier based orthogonal frequency division multiplexing (OFDM), extensively used in wireless communications, has been widely investigated in the super-channel transmission in optical communication systems to achieve spectral efficiency similar to that of Nyquist-spaced wavelength division multiplexing (WDM) [2]. Research in [3], [4] has compared typical OFDM and Nyquist-spaced WDM systems with the conclusion that, for the same optical bandwidth, both have the same bit-error-rate (BER) and transmission distance performance.

Two approaches can be applied to enhance the achievable spectral efficiency. One is to use higher-order modulation formats considering a given occupied bandwidth and the other is to occupy a smaller bandwidth by reducing sub-carrier spacing below the symbol rate, at the expense of a loss of orthogonality. Fast OFDM is an example of the latter technique which halves the occupied bandwidth but for specific set of modulation formats limited to real value (one dimensional) modulation and has been applied in various optical transmission systems [5], [6]. This paper, for the first time to our knowledge, reports a comparative study of these two approaches (higher-order modulation formats and sub-carrier spacing below the symbol rate) for optical transmission systems suffering fiber Kerr nonlinearities. The challenge in the first solution is the complexity and penalty of the generation of high-order modulation formats, and the challenge in the second solution is the inter-carrier interference (ICI) during the bandwidth compression [7]-[9]. Multicarrier systems can compress the bandwidth by adopting non-orthogonal multicarrier signals with sub-carrier spacing below the symbol rate, termed spectrally efficient frequency division multiplexing (SEFDM) [9]. A related technique termed faster than Nyquist (FTN) was reported in [10] where time domain techniques result in spectral efficiency improvement through sending data at rates faster than those

dictated by Nyquist. In previous reports, SEFDM has been investigated in short-distance optical fiber scenarios [11], [12], visible light communication (VLC) [13], optimum envelope investigations [14] and peak-to-average power ratio (PAPR) reduction [15].

All the work reported above showed the advantage of SEFDM in saving spectrum when compared to OFDM of the same modulation order, as well as the SEFDM error rate/power advantage when compared to OFDM of higher-order modulation but of the same spectral efficiency. However, no investigation for comparing the impact of fiber nonlinearities on SEFDM and OFDM systems has been reported. This work considers long-haul optical fiber communication scenarios where fiber nonlinearities have significant effects on signal performance, showing the achievable spectral efficiency and transmission distance limits of such optical communication systems.

2. Spectrally efficient frequency division multiplexing

The SEFDM signal consists of a stream of modulated SEFDM symbols each carrying *N* complex quadrature amplitude modulation (QAM) symbols [9], [14]. Each of the *N* complex symbols is modulated on one non-orthogonally packed sub-carrier. Therefore, the SEFDM signal can be expressed as:

$$x(t) = \frac{1}{\sqrt{T}} \sum_{l=-\infty}^{\infty} \sum_{n=0}^{N-1} S_{l,n} \exp\left[\frac{j2\pi n\alpha(t-lT)}{T}\right], \tag{1}$$

where α is the bandwidth compression factor defined as:

$$\alpha = \Delta f \cdot T, \tag{2}$$

where Δf denotes the frequency distance between adjacent subcarriers, T is the period of one SEFDM symbol, $1/\sqrt{T}$ is a scaling factor for the purpose of normalization, N is the number of sub-carriers and $S_{l,n}$ is the complex QAM symbol modulated on the n^{th} sub-carrier in the l^{th} SEFDM symbol. α determines the bandwidth compression and hence the percentage of bandwidth saving equals (1-α) × 100%. For OFDM signals α=1, and for SEFDM signal α<1. Figure 1 illustrates the spectra of OFDM and SEFDM signals. It is clearly seen that due to the non-orthogonal sub-carrier packing, SEFDM signal has a narrower bandwidth compared to the OFDM signal given the same number of sub-carriers and modulation bandwidth per sub-carrier, at the expense of self-created ICI.

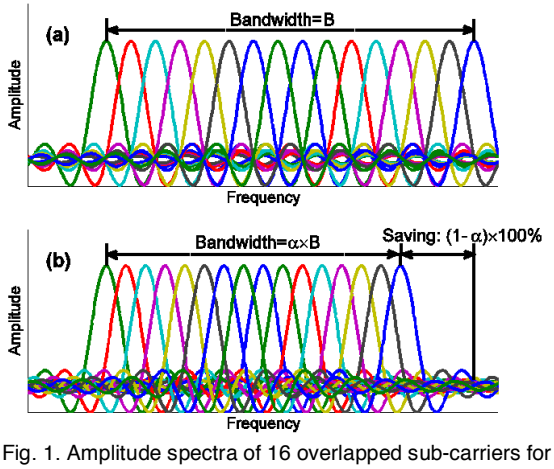

Fig. 1. Amplitude spectra of 16 overlapped sub-carriers for (a) OFDM and (b) SEFDM. Colors represent different sub-carriers to show the orthogonal overlapping in (a) and the non-orthogonal overlapping in (b).

SEFDM packs sub-carriers closer than OFDM leading to compressed signal bandwidth. In order to have a fair comparison within the same occupied signal bandwidth, SEFDM has to pack more sub-carriers. This is a method that can improve data rate to a level equivalent to higher-order modulation formats. For 4QAM modulated SEFDM signals, the sub-carrier packing scheme is shown in Table 1. The FFT size is 32 for all systems while the number of data sub-carriers is different in each system. The 4QAM modulated SEFDM signal packs five more sub-carriers than OFDM. However, the signal bandwidth is same for all systems but with higher symbol rate for SEFDM. Therefore, this leads to the same bit rate for 8QAM-OFDM and 4QAM-SEFDM signals. This table provides a possible way to replace higher-order modulation schemes with lower-order modulation formats. Note that here a dual-polarization signal transmission scheme, which could further double the system capacity, is considered in the optical fiber communication systems.

Table 1. 4QAM and 8QAM system specifications of dual-polarization OFDM and SEFDM (α=0.67)

Schemes	FFT size	Data sub-carriers	Bandwidth	Symbol rate	Bit rate
4QAM-OFDM	32	11	24 GHz	24 Gsymbol/s	96 Gbit/s
8QAM-OFDM	32	11	24 GHz	24 Gsymbol/s	144 Gbit/s
4QAM-SEFDM	32	16	24 GHz	36 Gsymbol/s	144 Gbit/s

For higher-order modulated SEFDM signals such as 16QAM, the bandwidth compression factor should be reconfigured and the number of extra sub-carriers is also reconfigured as shown in Table 2. The new system configurations lead to the same bit rate for 32QAM-OFDM and 16QAM-SEFDM, to allow fair comparisons.

Table 2. 16QAM and 32QAM system specifications of dual-polarization OFDM and SEFDM (α=0.8)

Schemes	FFT size	Data sub-carriers	Bandwidth	Symbol rate	Bit rate
16QAM-OFDM	32	11	24 GHz	24 Gsymbol/s	192 Gbit/s
32QAM-OFDM	32	11	24 GHz	24 Gsymbol/s	240 Gbit/s
16QAM-SEFDM	32	14	24 GHz	30 Gsymbol/s	240 Gbit/s

It is useful to represent the SEFDM signal in a discrete form for the purpose of signal analysis. A discrete signal is derived by sampling the first SEFDM symbol of Eq. (1) at T/Q intervals where $Q = \rho \cdot N$ and $\rho \geq 1$ is the oversampling factor. The discrete SEFDM signal for $k = [0, 1, ..., Q-1]$ is represented by:

$$X[k] = \frac{1}{\sqrt{Q}} \sum_{n=0}^{N-1} s_n \exp\left(\frac{j2\pi nk\alpha}{Q}\right), \tag{3}$$

where $X[k]$ is the k-th time sample of the first symbol of $x(t)$ in Eq. (1) and $1/\sqrt{Q}$ is a scaling factor, and s_n is the n-th QAM symbol. Furthermore, the signal can be simply expressed in a matrix form as:

$$X = \boldsymbol{F} \cdot S, \tag{4}$$

where X is a Q-dimensional vector of time samples of $x(t)$ in Eq. (1), S is an N-dimensional vector of transmitted symbols and $\boldsymbol{F}$ is a $Q \times N$ sampled sub-carrier matrix with elements equal to $\exp\left(\frac{j2\pi nk\alpha}{Q}\right)$.

3. SEFDM inter carrier interference analysis

At the receiver, X, defined in Eq. (4), is contaminated by the additive white Gaussian noise (AWGN) vector Z. The received signal is demodulated by correlating with the conjugate sub-carriers $\boldsymbol{F}^*$. The reception process is expressed as:

$$R = \boldsymbol{F}^* \cdot X + \boldsymbol{F}^* \cdot Z = \boldsymbol{F}^* \cdot \boldsymbol{F} \cdot S + \boldsymbol{F}^* \cdot Z = \boldsymbol{C} \cdot S + Z_{F^*}, \tag{5}$$

where R is an N-dimensional vector of demodulated symbols or in other words collected statistics, $\boldsymbol{C}$ is the $N \times N$ correlation matrix which is defined as $\boldsymbol{C} = \boldsymbol{F}^*\boldsymbol{F}$, where $\boldsymbol{F}^*$ denotes the $N \times Q$ conjugate sub-carrier matrix with elements equal to $\exp\left(\frac{-j2\pi nk\alpha}{Q}\right)$ for $k = [0, 1, ..., Q-1]$ and Z_{F^*} is the AWGN vector correlated with the conjugate sub-carriers. Interference from non-orthogonally packed sub-carriers can be defined by using the correlation matrix $\boldsymbol{C}$, where elements in the matrix is expressed as:

$$c_{m,n} = \frac{1}{Q} \times \begin{cases} Q & ,m = n \\ \dfrac{1-\exp\left[j2\pi\alpha(m-n)\right]}{1-\exp\left[j2\pi\alpha(m-n)/Q\right]} & ,m \neq n \end{cases}. \tag{6}$$

The detailed analysis of SEFDM interference can be found in work [16]. The interference caused by the off-diagonal ICI terms in the correlation matrix $\boldsymbol{C}$ can be evaluated by computing the cross-correlation between elements in the $\boldsymbol{C}$ matrix. Figure 2 illustrates three-dimensional plots of interference patterns for various systems. The numbers on the X-axis (indexed by X) and the Y-axis (indexed by Y) correspond to sub-carrier indices. Both x and y scale range from 0 to N-1. The X-Y plane indicates the correlation between sub-carriers. The numbers on the Z-axis (indexed by Z) indicate normalized absolute values of the correlation coefficients. It should be noted that the auto correlation coefficients are denoted by I(x, x) and the cross correlation coefficients are I(x, y) indicating ICI. For clarity of the figures the number of sub-carriers is limited to N=16 and the auto correlation elements are removed (i.e. I(x, x)=0), thereby only the cross correlation values are shown.

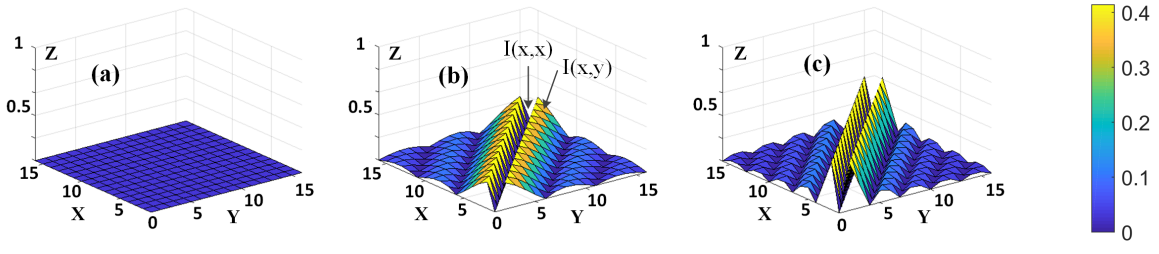

Fig. 2. Three-dimensional interference comparison. X and Y indicate sub-carrier indices and Z indicates normalized absolute correlation coefficients. (a) OFDM; (b) SEFDM α=0.8; (c) SEFDM α=0.67. The color bar indicates the scale of the interference.

Figure 2(a) expectedly shows no interference for the case of OFDM, and Fig. 2(b) illustrates an SEFDM system with 20% bandwidth compression (α=0.8). It is apparent that the interference is no longer zero and its values vary since sub-carriers

are no longer orthogonal. The interference levels clearly vary with the index (i.e. frequency location) of the sub-carriers with highest levels evident for adjacent sub-carriers (at the center of the X-Y plane). The interference in a higher bandwidth compressed SEFDM system with 33% bandwidth compression (α=0.67) is shown in Fig. 2(c), where higher levels are noticed (relative to the first two figures) as the sub-carriers become more tightly packed and therefore interfere with higher powers across the overall frequency band. Clearly, further bandwidth compression will result in more interference both from adjacent and non-adjacent sub-carriers.

4. Signal detection using sphere decoding

Unlike the case of OFDM signals, where simple linear detection followed by hard decision decoding results in optimum performance, the non-orthogonal nature of SEFDM dictates the use of complex non-linear detection methods. This loss of orthogonality between sub-carriers results in received signals severely affected by ICI, leading to increased error rates if linear detection is used. With the aim of reducing the error rate, maximum likelihood (ML) was firstly proposed as the optimal detection algorithm for SEFDM. The idea of ML is to search exhaustively over all the possible combinations of transmitted symbols (e.g. QAM) for each SEFDM symbol. The ML estimate of the received symbols in SEFDM can be expressed as:

$$S_{ML} = \arg\left\{\min_{S\in O^N} \|R - \boldsymbol{C}\cdot S\|^2\right\}, \tag{7}$$

where ||.|| denotes the Euclidean norm, S are the detected symbols, O is the constellation cardinality, N is the number of sub-carriers and therefore O^N is the set of all the possible symbol combinations. For a given received symbol, the optimum solution is the one that has the smallest Euclidean norm. Unfortunately, in practice, ML complexity increases greatly with the enlargement of the number of sub-carriers or the order of the modulation scheme. Therefore, ML is not considered as a practical solution.

To reduce the high complexity levels of the ML detection without compromising error rates, a complexity-reduced technique, termed sphere decoding (SD) [17] and initially proposed for use in multi-input multi-output (MIMO) systems, was successfully adapted to recover SEFDM signals with practical complexity [18]. The basic idea of sphere decoding is to achieve ML performance by searching for the best solution, being the smallest Euclidean norm, within a predefined sphere space which is constrained by an initial radius. Since the pre-defined search space is smaller than the infinite ML search space, sphere decoding achieves near optimum performance and significantly reduces receiver complexity.

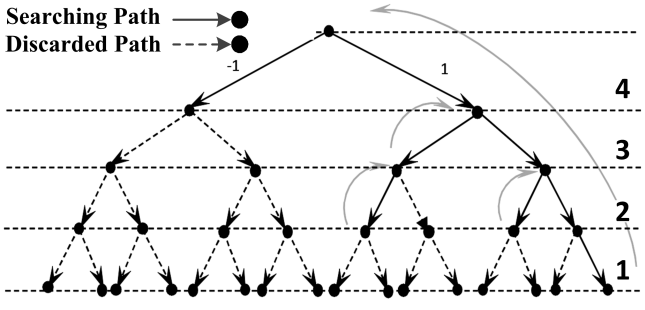

Fig. 3. SD tree search diagram for a 4 sub-carrier SEFDM signal with BPSK symbols.

Figure 3 illustrates a tree search diagram in order to show how the sphere decoding/ detection algorithm works. Each point in the tree is referred to as a node and simply represents a constellation point. The number of branches per node is equal to the constellation size (2 in this example). The number on the right at each level represents the index of sub-carriers in the SEFDM system (4 in this example). ML searches for all the nodes including both retained nodes and discarded nodes. However, SD only tests nodes within a predefined sphere space in Fig. 3. At each level, only points that within the sphere space are reserved while the rest of the nodes are discarded with all its predecessor nodes. The forward transition from a higher level to a lower level indicates the decision of one symbol; the backward transition (represented by a curved arrow) indicates the discard of one node and all its children nodes.

An initial radius determines the complexity of the decoding process since it determines the size of the search space. It is noted that a small radius will reduce the probability of finding the optimal solution since this limits the search space around a node while a large radius will increase the complexity. There are 31 nodes in Fig. 3. It is clearly seen that only 9 nodes are searched, while the rest of the nodes are discarded. Therefore, the throughput of sphere decoding is higher than that of ML and such throughput advantage will be more evident where higher modulation formats and/or a higher number of sub-carriers are employed. For a sphere decoder, search for the best estimate S_{SD} in SEFDM is defined as:

$$S_{SD} = \arg\left\{\min_{S\in O^N} \|R - \boldsymbol{C}\cdot S\|^2\right\} \le g, \tag{8}$$

where g is the initial radius which equals the distance between a demodulated symbol R and the initial constrained estimate S_{ZF} where S_{ZF} is the zero forcing estimate which can be obtained using the rounding function $\lfloor \cdot \rceil$ as $S_{ZF} = \lfloor \boldsymbol{C}^{-1} \cdot R \rceil$. Then the initial radius is set to be:

$$g = \left\| R - \boldsymbol{C} \cdot S_{ZF} \right\|^2 . \tag{9}$$

5. Optical transmission setup

The numerical SEFDM and OFDM transmission are implemented in a dual-polarization optical fiber communication system, as schematically shown in Fig. 4. At the transmitter for a given polarization, the bit stream is firstly mapped to M-QAM symbols and after serial/parallel conversion, frequency guard bands are added at both sides of the signal spectrum for the purpose of oversampling. Then, either OFDM or SEFDM IFFT is used to modulate the M-QAM symbols on each sub-carrier. After the parallel/serial conversion, the electrical signal complex representation is ideally mapped onto an optical carrier using the parameters given in Table 3. The same process is applied to the second polarization. Note that the modulated symbol sequences are independent and random for each polarization.

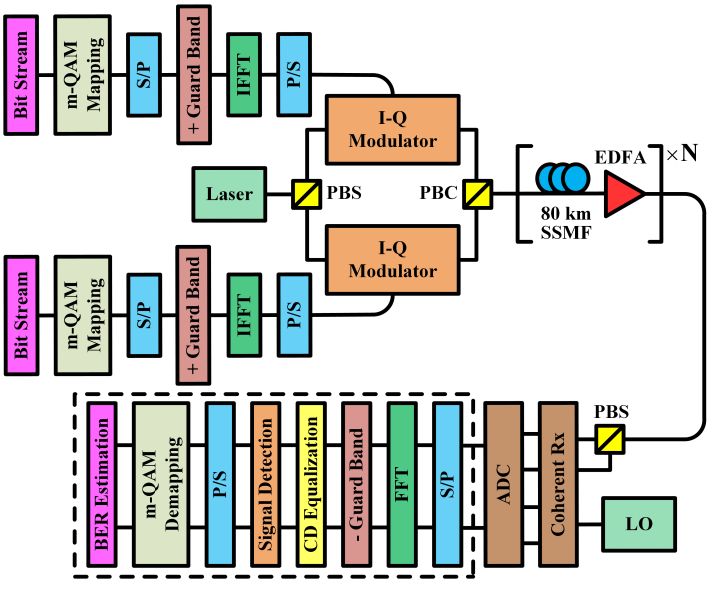

Fig. 4. Schematic of OFDM/SEFDM optical fiber transmission system. I-Q: in-phase and quadrature, S/P: serial to parallel, S/P: parallel to serial, PBS: polarization beam splitter, PBC: polarization beam combiner, Rx: receiver, ADC: analogue-to-digital converter.

The standard single-mode fiber (SSMF) is simulated by solving the Manakov equation using the split-step Fourier method with a logarithmic step-size distribution [19], [20]. An erbium-doped fiber amplifier (EDFA) is applied at the end of each transmission span to compensate for the fiber loss. At the receiver, the signal is mixed with an ideal local oscillator (LO) laser to implement phase- and polarization-diverse coherent detection. The detected signals are then digitized using ideal analogue-to-digital convertors. The system studied in this work does not employ cyclic prefix, and the chromatic dispersion (CD) was compensated using a frequency-domain equalizer [21], [22]. As the fiber dispersion is a linear effect, it can be fully compensated using digital signal processing (DSP) techniques in current long-haul optical fiber communication systems.

Table 3. System parameters

Parameters	Value
Transmission parameters	
Attenuation coefficient	0.2 dB/km
Chromatic dispersion coefficient	17 ps/(nm·km)
Nonlinear coefficient	1.2 /(W·km)
Span length	80 km
SSMF steps per span (logarithmic step size)	1000
EDFA noise figure	4.5 dB
Signal and modulation parameters	
Symbol rate	32 GBaud
Central wavelength (transmitter and LO)	1550 nm
Number of polarizations	2
Number of SEFDM/OFDM sub-carriers	16

The two digitized and compensated received signal samples (of the two polarizations) are processed in an identical manner. For each, the serial data is firstly converted to parallel (oversampled) multi-carrier (OFDM or SEFDM) symbol streams for the FFT demodulation operation. Then the frequency guard bands are removed to retrieve the M-QAM symbols for detection using either a zero-forcing detector or a sphere decoder. The receiver bit stream is obtained after parallel/serial conversion and M-QAM demapping. Finally, the system performance is assessed by estimating the BER with up to 10^6 bits (10,000 OFDM or SEFDM symbols on each polarization). All simulations are implemented with an oversampling factor equals two. The frequency offset and phase noise in the transmitter and LO lasers and the differential group delay between two polarizations in the optical fiber are neglected. Transmission system parameters are detailed in Table 3.

6. Results and discussions

For binary symmetric channels where binary input/output and symmetric transition probability are applied, the coding rate R_C in the M-QAM optical fiber communication systems, assuming an ideal hard-decision forward error correction (FEC) code, can be calculated according to the achievable pre-FEC BER [23], [24]:

$$R_C = 1 + BER \cdot \log_2 BER + (1 - BER) \cdot \log_2 (1 - BER). \tag{10}$$

Therefore, the achievable spectral efficiency can be computed accordingly as:

$$SE = \frac{1}{\alpha} \cdot R_C \cdot N_P \cdot \log_2 M, \tag{11}$$

where *SE* is the achievable spectral efficiency, *M* is the constellation size and N_P is the number of polarization states. The comparison of *SE* values, for SEFDM and OFDM is shown in Table 4.

Table 4. Ideal and achievable spectral efficiency of dual-polarization OFDM and SEFDM

Schemes	Ideal spectral efficiency	Achievable spectral efficiency at BER=3.8×10^{-3}
4QAM-OFDM	4 bit/(s·Hz)	3.86 bit/(s·Hz)
8QAM-OFDM	6 bit/(s·Hz)	5.78 bit/(s·Hz)
4QAM-SEFDM (α=0.67)	6 bit/(s·Hz)	5.78 bit/(s·Hz)
16QAM-OFDM	8 bit/(s·Hz)	7.712 bit/(s·Hz)
32QAM-OFDM	10 bit/(s·Hz)	9.64 bit/(s·Hz)
16QAM-SEFDM (α=0.8)	10 bit/(s·Hz)	9.64 bit/(s·Hz)

We observe that 4QAM-SEFDM can ideally achieve the same spectral efficiency as 8QAM-OFDM and at the same time shows 50% spectral efficiency gain over 4QAM-OFDM. This indicates a possible route to replace high-order modulation formats with lower-order ones.

As mentioned in [3], [4], conventional OFDM and Nyquist-spaced WDM systems have the same nonlinear performance in both single-channel and multi-channel transmissions. An optical communication system was implemented to investigate the efficiency of SEFDM signal transmission over long-haul fibers, compared to conventional OFDM signals. Firstly, an optical fiber with length of 7200 km (90×80 km) was evaluated. Sphere decoding was used to recover 4QAM-SEFDM signals from the self-created ICI at the receiver, showing much improved performance over the zero-forcing (ZF) detector, which can be used in OFDM systems, as shown in Fig. 5. It is clearly seen that by employing sphere decoding (SEFDM-SD curve) the FEC threshold of BER=3.8×10^{-3} can be reached, allowing the transmission over 7200 km fiber. Given the significant outperformance relative to the zero-forcing detection, only sphere decoding will be used for SEFDM transmission in the following simulations.

SEFDM is a non-orthogonal waveform that introduces interference between sub-carriers, which doesn't exist in OFDM. Therefore, an interference cancellation-based receiver has to be used for SEFDM. The use of sphere decoding for OFDM signals cannot improve its BER performance since there is no self-created ICI within OFDM signals. Sphere decoding can only take effect for ICI affected signals such as SEFDM.

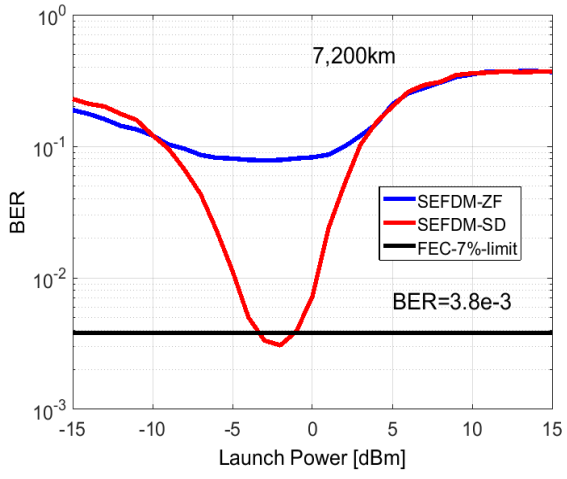

Fig. 5. BER versus optical launch power for two 4QAM-SEFDM (α=0.67) signal detectors at a transmission distance of 7200 km. ZF: zero-forcing, SD: sphere decoding.

In order to show the benefits of SEFDM over OFDM, three systems of the same signal bandwidth tested with two different modulation formats over 7200 km fiber, are compared in Fig. 6(a). 4QAM and 8QAM symbols were applied for OFDM while only 4QAM was applied for SEFDM. As shown in Table 4, to achieve the same spectral efficiency as the 8QAM-OFDM, the 4QAM-SEFDM bandwidth compression factor α value must be set to 0.67, resulting in 33% bandwidth reduction or 50% improvement of spectral efficiency. Since the 4QAM-SEFDM and the 8QAM-OFDM have the same spectral efficiency and occupy the same bandwidth, thus, they both have the same data rate. However, for the dual-polarization 4QAM-OFDM signal, the spectral efficiency takes the lower value of 3.86 bit/(s·Hz). Considering the same occupied signal bandwidth, the 4QAM-OFDM signal has a reduced data rate (by 50%) when compared to 4QAM-SEFDM and 8QAM-OFDM rates.

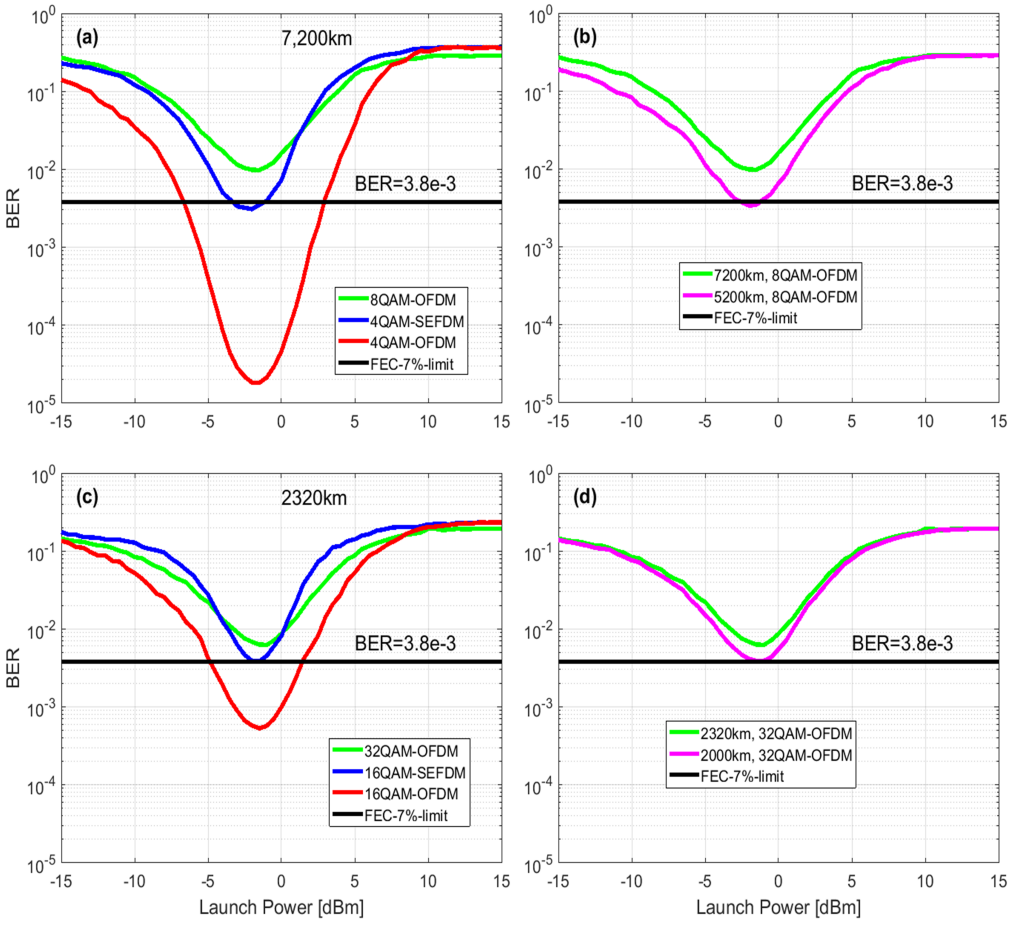

Fig. 6. BER versus optical launch power for OFDM and SEFDM. (a) 8QAM-OFDM, 4QAM-SEFDM and 4QAM-OFDM systems at a transmission distance of 7200 km. (b) 8QAM-OFDM systems at transmission distances of 5200 km and 7200 km. (c) 32QAM-OFDM, 16QAM-SEFDM and 16QAM-OFDM systems at a transmission distance of 2320 km. (d) 32QAM-OFDM systems at transmission distances of 2320 km and 2000 km.

It is clearly seen that three curves have nearly the same optimal launch power (~ -2 dBm) due to the same occupied bandwidth. The 4QAM modulated OFDM signal can reach the FEC limit and cross the threshold at two launch power points (-7 dBm and 3 dBm, respectively). The 4QAM modulated SEFDM signal just approaches the FEC limit with the crossing point being approximately -2 dBm. However, for the 8QAM modulated OFDM signal, it is above the FEC threshold and will never cross it. The comparison in Fig. 6(a) is focused on the 4QAM-SEFDM and the 8QAM-OFDM signals due to their identical signal bandwidth, spectral efficiency and data rate. Based on the aforementioned results, it is inferred that the 4QAM modulated SEFDM signal can reach 7200 km distance while its spectral efficiency equivalent, the 8QAM modulated OFDM signal will not achieve such transmission distance. The 4QAM-OFDM signal shows the best performance due to the fact that the number of sub-carriers is smaller and the constellation density is lower, resulting in lower levels of interference.

The maximum transmission distance of 8QAM-OFDM for a target BER of 3.8×10^{-3} was studied and plotted in Fig. 6(b). The distance is decreased gradually and when 5200 km is configured for the 8QAM-OFDM system, the performance curve just crosses the BER threshold with the optimal launch power being approximately -2 dBm. This indicates that the maximum distance that can be reached by 8QAM-OFDM signal is 5200 km. Thus, compared to 4QAM-SEFDM signal, at the same spectral efficiency, same bandwidth and same data rate, the use of 4QAM-SEFDM results in ~38.5% improvement of transmission distance.

For higher order modulation formats (16QAM and 32QAM), results are shown in Fig. 6(c) and Fig. 6(d) where three systems are demonstrated. Figure 6(c) shows that the 16QAM-SEFDM performance can reach 3.8×10^{-3} at a distance of 2320 km while the 32QAM-OFDM cannot reach such a distance. Since both OFDM and SEFDM signals occupy the same bandwidth, the optimal launch power here is again identical, which is -2 dBm. The 16QAM-OFDM has the best performance crossing the FEC limit at the launch powers of -5 dBm and 1.5 dBm at BER=3.8×10^{-3}. However, for the 32QAM-OFDM signal, it cannot reach the FEC threshold. An interesting finding is that the 16QAM-SEFDM system behaves worse than the 32QAM-OFDM system at both linear and strong nonlinear regimes, but it performs better than the 32QAM-OFDM system around their optimum power regions. This leads to the overall outperformance of the 16QAM-SEFDM. For the high-density constellations, the sphere decoding cannot effectively remove the ICI within SEFDM signals with the existence of strong noise, but it can work well with reduced noise (in the regime around optimum power). The reason is that the performance of the sphere decoding detector in the SEFDM is very sensitive to noise as explained in [25]. Basically, with strong noise power, zero forcing estimate S_{ZF} is not accurate leading to an imperfect SD decision initial radius in Eq. (9), which will further affect the performance of SD detection in Eq. (8). However, in low noise conditions, SD can fully show its ability in removing the ICI. Similar phenomena have also been found in the reported work [26]. In order to evaluate the maximum transmission distance for 32QAM-OFDM signal, Fig. 6(d) presents two systems operating at two fiber distances. It is therefore clear that the maximum reach of 32QAM-OFDM signal is approximately 2000 km.

In this work, we compare systems of equal spectral efficiencies and information rates. Although the optical spectrum is compressed resulting in higher levels of interference, operation in the optimal launch power shows significant BER improvement for 4QAM-SEFDM and 16QAM-SEFDM when compared to their respective spectrally equivalent 8QAM-OFDM and 32QAM-OFDM. The reason of the improved BER performance is explained by considering the Euclidean distance for a given constellation, which is maintained in SEFDM, even with its increased ICI, up till a value of α=0.8, as predicted by Mazo's 1975 work of [10]. Although this distance is compromised with higher compression, the fact that the ICI in SEFDM is deterministic as explained in [16] makes it possible to allow amelioration of ICI effects at the receiver and maintain only a slight degradation of the Euclidian distance before hard decision is applied, at the signal detection stage, which, in this work, uses the sphere decoder. This explains why SEFDM shows satisfactory BER performance even with its compressed bandwidth. Meanwhile, the use of sphere decoding, which can greatly reduce the effects of interference created within SEFDM signals, results in near optimum performance approaching that of the more complex yet optimum maximum likelihood performance. These aspects contribute to the extended transmission distance by lowering the BER value for SEFDM signals relative to OFDM ones at the optimal launch power.

To provide a more comprehensive investigation on the broadband transmission, the performance of SEFDM system has also been studied compared to the performance of a 5-channel 32-Gbaud Nyquist-spaced WDM system, where the transmission distance is 1760 km (22×80 km) and the system bandwidth is 160 GHz. To design a fair comparison, a modulation format of 32QAM is employed in the 5-channel WDM system and a 16QAM is used in the SEFDM system where the full bandwidth (160 GHz) is filled by SEFDM signals with α=0.8. Both systems have an ideal spectral efficiency of 10 bit/(s·Hz) and and ideal transmission speed of 1.6 Tbit/s. Simulation results are illustrated in Figure 7. The green curve represents the average BER performance for the 5-channel WDM system (average BER over 5 channels), and the blue curve represents the behavior of the SEFDM transmission system. It can be found that for the same transmission distance (1760 km) the SEFDM signal shows a better performance compared to the 5-channel WDM transmission. The SEFDM transmission has its lowest BER value of 3.19×10^{-3} at an optimum launch power of -4.3 dBm, and the 5-channel WDM transmission has its lowest BER value of 6.06×10^{-3} at an optimum launch power of -4.5 dBm, which almost doubled the error rate compared to the SEFDM system.

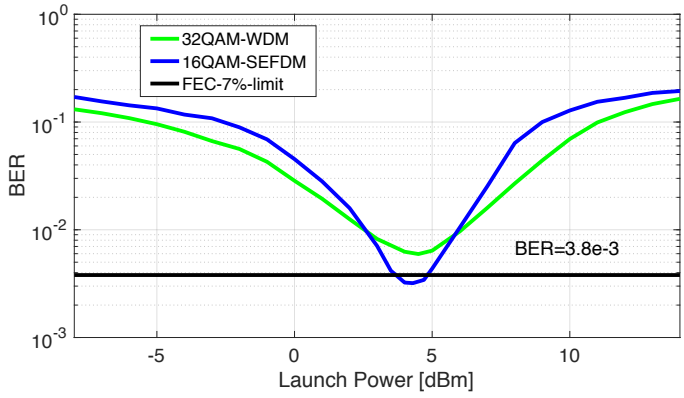

Fig. 7. BER versus optical launch power for multi-channel WDM and SEFDM systems at a transmission distance of 1760 km.

In order to analyze further the cause of the benefits using SEFDM signals, peak-to-average power ratio (PAPR) was evaluated for both OFDM and SEFDM signals. The complementary cumulative distribution function was used as a way to analyze the probability of PAPR being higher than a predefined threshold γ. Fig. 8 presents two schemes: the OFDM signal and the SEFDM signal with α=0.67. Results in Fig. 8 show that although the bandwidth was compressed in the SEFDM signal, the probability of the PAPR exceeding the threshold γ is similar to that of the OFDM signal, indicating that the PAPR has the same effect in both systems.

It is noted that compared to OFDM using higher-order modulation formats, SEFDM signal with lower modulation format performs better at the optimal launch power. This indicates the SEFDM will be more effective in increasing the maximum reach of optical communication systems, when the nonlinearity compensation [20,27] is applied. The SD is a compromise solution with performance superior to that of ZF, which is the least complex of detection methods, yet approaching the optimum performance of ML but with a much lower complexity. It is worth mentioning that the SD has a variable complexity, which has been analyzed in previous work [25], [28]. The complexity of SD is generally measured via "number of visited nodes" and is highly dependent on the signal-to-noise ratio (SNR). At a lower SNR range (i.e. higher noise power), more nodes have to be visited in the SD, which indicates a higher complexity of SD. However, with the increase of SNR, the number of visited nodes in SD detection is reduced, which indicates a lower complexity of SD. Since the transmission is operated around optimum signal launch powers in practical systems, the complexity of the SD is generally acceptable at such an optimum SNR range which indicates the feasibility of the SEFDM transmission scheme.

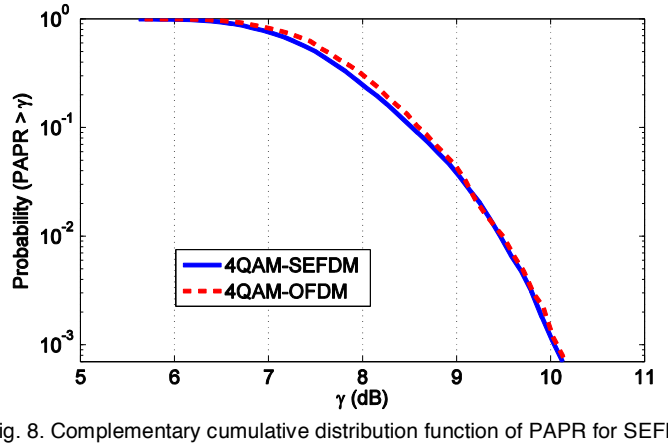

Fig. 8. Complementary cumulative distribution function of PAPR for SEFDM and OFDM signals modulated with 4QAM symbols.

7. Conclusions

This paper has investigated the predicted performance of orthogonal (OFDM) and non-orthogonal (SEFDM) multicarrier systems in long-haul optical fiber transmission environments where fiber nonlinearities are considered. SEFDM, which can improve the spectral efficiency by packing subcarriers closer than in OFDM shows advantages over OFDM when the signals are transmitted over nonlinear optical fibers. When considering systems of the same achievable spectral efficiency and bit rate (4QAM-SEFDM with α=0.67 and 8QAM-OFDM; 16QAM-SEFDM with α=0.8 and 32QAM-OFDM) and for a FEC limit of 3.8×10^{-3}; the 4QAM-SEFDM signal has ~38.5% reach advantage extending transmission distance to 7200 km while the 8QAM-OFDM signal can only reach 5200 km. For higher order modulation formats, 16QAM-SEFDM outperforms a spectrally equivalent 32QAM-OFDM by 16%. Our work demonstrates that the use of SEFDM signals can potentially increase the transmission distance of optical transmission systems and that such increase is expected to be more significant if the nonlinearity compensation is applied.

In the future work, the application of the nonlinearity compensation in SEFDM optical transmission systems will be investigated, where the digital back-propagation algorithm will be employed to compensate for both intra-channel (self-phase modulation) and inter-channel (cross-phase modulation and four-wave mixing) fiber nonlinearities [27], [29]. As it has been found that the sphere decoding cannot effectively remove the ICI in the strong nonlinear regime which leads to a suboptimal operation of SEFDM signals, the mitigation of fiber nonlinearities using the digital back-propagation is also expected to further improve the suppression of ICI in SEFDM optical transmission systems. In addition, experiments for verifying the advantage of the SEFDM transmission over nonlinear optical fiber channels will also be carried out.

Acknowledgements

The authors would like to thank Dr. Domaniç Lavery from UCL for helpful discussions.

References

[1] P. J. Winzer, "High-spectral-efficiency optical modulation formats," J. Lightwave Technol., vol. 30, no. 24, pp. 3824-3835, 2012.
[2] S. Chandrasekhar, X. Liu, B. Zhu, and D. W. Peckham, "Transmission of a 1.2-Tb/s 24-carrier no-guard-interval coherent OFDM superchannel over 7200-km of ultra-large-area fiber, in Proc. IEEE Eur. Conf. Opt. Commun., 2009, pp. PD2.6.
[3] G. Bosco, A. Carena, V. Curri, P. Poggiolini, and F. Forghieri, "Performance limits of Nyquist-WDM and CO-OFDM in high-speed PM-QPSK systems," IEEE Photon. Technol. Lett., vol. 22, no. 15, pp. 1129-1131, 2010.
[4] S. Kilmurray, T. Fehenberger, P. Bayvel, and R. I. Killey, "Comparison of the nonlinear transmission performance of quasi-Nyquist WDM and reduced guard interval OFDM," Opt. Express, vol. 20, no. 4, pp. 4198-4205, 2012.
[5] M. R. D. Rodrigues and I. Darwazeh, "Fast OFDM: a proposal for doubling the data rate of OFDM schemes," in Proc. IEEE Int. Conf. Telecommun., 2002, pp. 484-487.
[6] J. Zhao and A. D. Ellis. "A novel optical fast OFDM with reduced channel spacing equal to half of the symbol rate per carrier," in Proc. IEEE Opt. Fiber Commun. Conf., 2010, pp. OMR1.
[7] P. J. Winzer and R.-J. Essiambre, "Advanced modulation formats for high-capacity optical transport networks," J. Lightwave Technol., vol. 24, no. 12, pp. 4711-4728, 2006.
[8] L. Tao, Y. Ji, J. Liu, A. P. T. Lau, N. Chi, and C. Lu, "Advanced modulation formats for short reach optical communication systems," IEEE Netw., vol. 27, no. 6, pp. 6-13, 2013.
[9] M. Rodrigues and I. Darwazeh, "A spectrally efficient frequency division multiplexing based communications system," in Proc. 8th IEEE Int. OFDM-Workshop, 2003, pp. 48-49.
[10] J. Mazo, "Faster-than-Nyquist signaling," Bell Syst. Tech. J., vol. 54, no. 8, pp. 1451-1462, 1975.
[11] D. Nopchinda, T. Xu, R. Maher, B. Thomsen, and I. Darwazeh, "Dual polarization coherent optical spectrally efficient frequency division multiplexing," IEEE Photon. Technol. Lett., vol. 28, no. 1, pp. 83-86, 2016.
[12] T. Xu, S. Mikroulis, J. E. Mitchell, and I. Darwazeh, "Bandwidth compressed waveform for 60-GHz millimeter-wave radio over fiber experiment," J. Lightwave Technol., vol. 34, no. 14, pp. 3458-3465, 2016.
[13] Y. Wang, Y. Zhou, T. Gui, K. Zhong, X. Zhou, L. Wang, A. P. T. Lau, C. Lu, and N. Chi, "SEFDM based spectrum compressed VLC system using RLS time-domain channel estimation and ID-FSD hybrid decoder," in Proc. IEEE Eur. Conf. Opt. Commun., 2016, pp. 827-829.
[14] S. V. Zavjalov, S. V. Volvenko, and S. B. Makarov, "A method for increasing the spectral and energy efficiency SEFDM signals," IEEE Commun. Lett., vol. 20, no. 12, pp. 2382-2385, 2016.
[15] E. O. Antonov, A. V. Rashich, D. K. Fadeev, and N. Tan, "Reduced complexity tone reservation peak-to-average power ratio reduction algorithm for SEFDM signals," in Proc. 39th IEEE Int. Conf. Telecommun. Signal Process., 2016, pp. 445-448.
[16] S. Isam and I. Darwazeh, "Characterizing the intercarrier interference of non-orthogonal spectrally efficient FDM system," in Proc. 8th IEEE Int. Symp. Commun. Syst., Netw. Digital Sig. Process., 2012, pp. 1-5.
[17] B. Hassibi and H. Vikalo, "On the sphere-decoding algorithm I. expected complexity," IEEE Trans. Signal Process., vol. 53, no. 8, pp. 2806-2818, 2005.
[18] I. Kanaras, A. Chorti, M. Rodrigues, and I. Darwazeh, "A fast constrained sphere decoder for ill conditioned communication systems," IEEE Commun. Lett., vol. 14, no. 11, pp. 999-1001, 2010.
[19] G. Bosco, A. Carena, V. Curri, R. Gaudino, P. Poggiolini, and S. Benedetto, "Suppression of spurious tones induced by the split-step method in fiber systems simulation," IEEE Photon. Technol. Lett., vol. 12, no. 5, pp. 489-491, 2000.
[20] T. Xu, N. A. Shevchenko, D. Lavery, D. Semrau, G. Liga, A. Alvarado, R. I. Killey, and P. Bayvel, "Modulation format dependence of digital nonlinearity compensation performance in optical fibre communication systems," Opt. Express, vol. 25, no. 4, pp. 3311-3326, 2017.
[21] S. J. Savory, "Digital filters for coherent optical receivers," Opt. Express, vol. 16, no. 2, pp. 804-817, 2008.
[22] R. Kudo, T. Kobayashi, K. Ishihara, Y. Takatori, A. Sano, and Y. Miyamoto, "Coherent optical single carrier transmission using overlap frequency domain equalization for long-haul optical systems," J. Lightwave Technol., vol. 27, no. 16, pp. 3721-3728, 2009.
[23] T. M. Cover and J. A. Thomas, Elements of Information Theory, 2nd ed., John Wiley & Sons, Inc., 2006.
[24] S. J. Savory, "Congestion aware routing in nonlinear elastic optical networks," IEEE Photon. Technol. Lett., vol. 26, no. 10, pp. 1057-1060, 2014.
[25] S. Isam, Spectrally efficient FDM communication signals and transceivers: design, mathematical modeling and system optimization, University College London PhD thesis, 2011.
[26] T. Xu and I. Darwazeh, "Multi-sphere decoding of block segmented SEFDM signals with large number of sub-carriers and high modulation order," in Proc. Int. Conf. Wirel. Netw. Mob. Commun., 2017, pp. 1-6.
[27] E. M. Ip and J. M. Kahn, "Compensation of dispersion and nonlinear impairments using digital backpropagation," J. Lightwave Technol., vol. 26, no. 20, pp. 3416-3425, 2008.
[28] I. Kanaras, A. Chorti, M. Rodrigues, and I. Darwazeh, "Spectrally efficient FDM signals: bandwidth gain at the expense of receiver complexity," in Proc. IEEE Int. Conf. Commun., 2009, pp. 1-6.
[29] G. Liga, T. Xu, A. Alvarado, R. I. Killey, and P. Bayvel, "On the performance of multichannel digital backpropagation in high-capacity long-haul optical transmission," Opt. Express, vol. 22, no. 24, pp. 30053-30062, 2014.